Quantum Phase Transitions

Subir Sachdev
Department of Physics
Yale University
P.O. Box 208120, New Haven, CT 06520-8120
USA
E-mail: subir.sachdev@yale.edu

May 19, 2004

To appear in **Encyclopedia of Mathematical Physics**, edited by J.-P. Françoise, G. Naber, and T. S. Tsun, Elsevier.

1 Introduction

The study of second-order phase transitions at nonzero temperatures has a long and distinguished history in statistical mechanics. Many key physical phenomena, such as the loss of ferromagnetism in iron at the Curie temperature or the critical end-point of CO_2, are now understood in precise quantitative detail. This understanding began in the work of Onsager, and is based upon what may now be called the Landau-Ginzburg-Wilson theory. The content of this sophisticated theory may be summarized in a few basic principles: (a) The collective thermal fluctuations near second-order transitions can be accurately described by simple classical models *i.e.* quantum-mechanical effects can be entirely neglected. (b) The classical models identify an *order parameter*, a collective variable which has to be treated on par with other thermodynamic variables, and whose correlations exhibit distinct behavior in the phases on either side of the transition. (c) The thermal fluctuations of the order parameter near the transition are controlled by a continuum field

theory whose structure is usually completed dictated by simple symmetry considerations.

This article will *not* consider such non-zero temperature phase transitions, but will instead describe second-order phase transitions at the absolute zero of temperature. Such transitions are driven by quantum fluctuations mandated by the Heisenberg uncertainty principle: one can imagine moving across the quantum critical point by effectively "tuning the value of Planck's constant, $\hbar$". Clearly quantum mechanics plays a central role at such transitions, unlike the situation at non-zero temperatures. The reader may object that absolute zero is an idealization not realized by any experimental system, and hence the study of quantum phase transitions is a subject only of academic interest. As we will illustrate below, knowledge of the zero temperature quantum critical points of a system is often the key to understanding its finite temperature properties, and in some cases the influence of a zero temperature critical point can be detected at temperatures as high as ambient room temperature.

We will begin in Section 2 by introducing some simple lattice models which exhibit quantum phase transitions. The theory of the critical point in these models is based upon a natural extension of the Landau-Ginzburg-Wilson (LGW) method, and this will be presented in Section 3. This section will also describe the consequences of a zero temperature critical point on the non-zero temperature properties. Section 4 will consider more complex models in which quantum interference effects play a more subtle role, and which cannot be described in the LGW framework: such quantum critical points are likely to play a central role in understanding many of the correlated electron systems of current interest.

2 Simple models

2.1 Quantum Ising chain

This is a simple model of N qubits, labeled by the index $j = 1 \ldots N$. On each 'site' j there two qubit quantum states $|\uparrow\rangle_j$ and $|\downarrow\rangle_j$ (in practice, these could be 2 magnetic states of an ion at site j in a crystal). The Hilbert space therefore consists of 2^N states, each consisting of a tensor product of

the states on each site. We introduce the Pauli spin operators, $\hat{\sigma}_j^\alpha$, on each site j, with $\alpha = x, y, z$:

$$\hat{\sigma}^x = \begin{pmatrix} 0 & 1 \\ 1 & 0 \end{pmatrix} \;\; ; \;\; \hat{\sigma}^y = \begin{pmatrix} 0 & -i \\ i & 0 \end{pmatrix} \;\; ; \;\; \hat{\sigma}^z = \begin{pmatrix} 1 & 0 \\ 0 & -1 \end{pmatrix}. \tag{1}$$

These operators clearly act on the 2 states of the qubit on site j, and the Pauli operators on different sites commute.

The quantum Ising chain is defined by the simple Hamiltonian

$$H_I = -J \sum_{j=1}^{N-1} \hat{\sigma}_j^z \hat{\sigma}_{j+1}^z - gJ \sum_{j=1}^{N} \hat{\sigma}_j^x, \tag{2}$$

where $J > 0$ sets the energy scale, and $g \geq 0$ is a dimensionless coupling constant. In the thermodynamic limit ($N \to \infty$), the ground state of H_I exhibits a second-order quantum phase transition as g is tuned across a critical value $g = g_c$ (for the specific case of H_I it is known that $g_c = 1$), as we will now illustrate.

First, consider the ground state of H_I for $g \ll 1$. At $g = 0$, there are two degenerate *ferromagnetically ordered* ground states

$$|\Uparrow\rangle = \prod_{j=1}^{N} |\uparrow\rangle_j \;\; ; \;\; |\Downarrow\rangle = \prod_{j=1}^{N} |\downarrow\rangle_j \tag{3}$$

Each of these states breaks a discrete 'Ising' symmetry of the Hamiltonian– rotations of all spins by 180 degrees about the x axis. These states are more succinctly characterized by defining the ferromagnetic moment, N_0 by

$$N_0 = \langle \Uparrow | \, \hat{\sigma}_j^z \, | \Uparrow \rangle = - \langle \Downarrow | \, \hat{\sigma}_j^z \, | \Downarrow \rangle \tag{4}$$

At $g = 0$ we clearly have $N_0 = 1$. A key point is that in the thermodynamic limit, this simple picture of the ground state survives for a finite range of small g (indeed, for all $g < g_c$), but with $0 < N_0 < 1$. The quantum tunnelling between the two ferromagnetic ground states is exponentially small in N (and so can be neglected in the thermodynamic limit), and so the ground state remains two-fold degenerate and the discrete Ising symmetry remains broken. The change in the wavefunctions of these states from Eq. (3) can be easily determined by perturbation theory in g: these small g quantum fluctuations

reduce the value of N_0 from unity but do not cause the ferromagnetism to disappear.

Now consider the ground state of H_I for $g \gg 1$. At $g = \infty$ there is a single *non*-degenerate ground state which fully preserves all symmetries of H_I:

$$|\Rightarrow\rangle = 2^{-N/2} \prod_{j=1}^{N} \left(|\uparrow\rangle_j + |\downarrow\rangle_j \right). \tag{5}$$

It is easy to verify that this state has no ferromagnetic moment $N_0 = \langle\Rightarrow| \hat{\sigma}_j^z |\Rightarrow\rangle = 0$. Further, perturbation theory in $1/g$ shows that these features of the ground state are preserved for a finite range of large g values (indeed, for all $g > g_c$). One can visualize this ground state as one in which strong quantum fluctuations have destroyed the ferromagnetism, with the local magnetic moments quantum tunnelling between 'up' and 'down' on a time scale of order $\hbar/J$.

Given the very distinct signatures of the small g and large g ground states, it is clear that the ground state cannot evolve smoothly as a function of g. These must be at least one point of non-analyticity as a function of g: for H_I it is known that there is only a single non-analytic point, and this is at the location of a second-order quantum phase transition at $g = g_c = 1$.

The character of the excitations above the ground state also undergoes a qualitative change across the quantum critical point. In both the $g < g_c$ and $g > g_c$ phase these excitations can be described in the Landau *quasiparticle* scheme *i.e.* as superpositions of nearly independent particle-like excitations; a single well-isolated quasiparticle has an infinite lifetime at low excitation energies. However, the physical nature of the quasiparticles is very different in the two phases. In the ferromagnetic phase, with $g < g_c$, the quasiparticles are domain walls between regions of opposite magnetization:

$$|j, j+1\rangle = \prod_{k=1}^{j} |\uparrow\rangle_k \prod_{\ell=j+1}^{N} |\downarrow\rangle_\ell \tag{6}$$

This is the exact wavefunction of a stationary quasiparticle excitation between sites j and $j+1$ at $g = 0$; for small non-zero g the quasiparticle acquires a 'cloud' of further spin-flips and also becomes mobile. However the its qualitative interpretation as a domain wall between the two degenerate ground states remains valid for all $g < g_c$. In contrast, for $g > g_c$, there is no

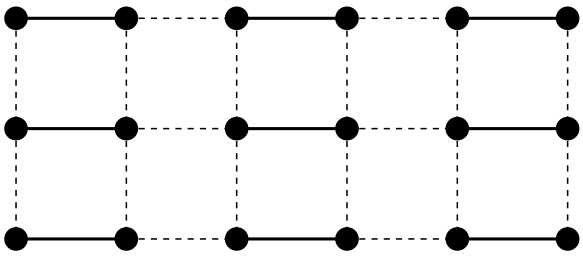

Figure 1: The coupled dimer antiferromagnet. Qubits (*i.e.* $S = 1/2$ spins) are placed on the sites, the $\mathcal{A}$ links are shown as full lines, and the $\mathcal{B}$ links as dashed lines.

ferromagnetism, and the non-degenerate paramagnetic state has a distinct quasiparticle excitation:

$$|j\rangle = 2^{-N/2}\left(|\uparrow\rangle_j - |\downarrow\rangle_j\right)\prod_{k\neq j}\left(|\uparrow\rangle_k + |\downarrow\rangle_k\right). \tag{7}$$

This is a stationary 'flipped spin' quasiparticle at site j, with its wavefunction exact at $g = \infty$. Again, this quasiparticle is mobile and applicable for all $g > g_c$, but there is no smooth connection between Eq. (7) and (6).

2.2 Coupled dimer antiferromagnet

This model also involves qubits, but they are now placed on the sites, j, of a two-dimensional square lattice. Models in this class describe the magnetic excitations of many experimentally important spin gap compounds.

The Hamiltonian of the dimer antiferromagnet is illustrated in Fig 1 and is given by

$$\begin{aligned} H_d &= J\sum_{\langle jk\rangle\in A}\left(\hat{\sigma}_j^x\hat{\sigma}_k^x + \hat{\sigma}_j^y\hat{\sigma}_k^y + \hat{\sigma}_j^z\hat{\sigma}_k^z\right) \\ &+ \frac{J}{g}\sum_{\langle jk\rangle\in B}\left(\hat{\sigma}_j^x\hat{\sigma}_k^x + \hat{\sigma}_j^y\hat{\sigma}_k^y + \hat{\sigma}_j^z\hat{\sigma}_k^z\right), \end{aligned} \tag{8}$$

where $J > 0$ is the exchange constant, $g \geq 1$ is the dimensionless coupling, and the set of nearest-neighbor links $\mathcal{A}$ and $\mathcal{B}$ are defined in Fig 1. An important property of H_d is that it is now invariant under the full O(3)

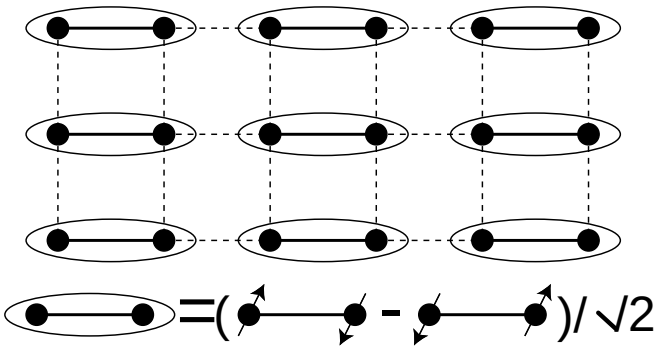

Figure 2: The paramagnetic state of H_d for $g > g_c$. The state illustrated is the exact ground state for $g = \infty$, and it is adiabatically connected to the ground state for all $g > g_c$.

group of spin rotations under which the $\hat{\sigma}^\alpha$ transform as ordinary vectors (in contrast to the Z_2 symmetry group of H_I). In analogy with H_I, we will find that H_d undergoes a quantum phase transition from a paramagnetic phase which preserves all symmetries of the Hamiltonian at large g, to an *antiferromagnetic* phase which breaks the O(3) symmetry at small g. This transition occurs at a critical value $g = g_c$, and the best current numerical estimate is $1/g_c = 0.52337(3)$.

As in the previous section, we can establish the existence of such a quantum phase transition by contrasting the disparate physical properties at large g with those at $g \approx 1$. At $g = \infty$ the exact ground state of H_d is

$$|\text{spin gap}\rangle = \prod_{\langle jk\rangle \in A} \frac{1}{\sqrt{2}} \left(|\uparrow\rangle_j |\downarrow\rangle_k - |\downarrow\rangle_j |\uparrow\rangle_k \right) \tag{9}$$

and is illustrated in Fig 2. This state is non-degenerate and invariant under spin rotations, and so is a paramagnet: the qubits are paired into spin singlet valence bonds across all the $\mathcal{A}$ links. The excitations above the ground state are created by breaking a valence bond, so that the pair of spins form a spin triplet with total spin $S = 1$ — this is illustrated in Fig 3. It costs a large energy to create this excitation, and at finite g the triplet can hop from link to link, creating a gapped *triplon* quasiparticle excitation. This is similar to the large g paramagnet for H_I, with the important difference that each quasiparticle is now 3-fold degenerate.

At $g = 1$, the ground state of H_d is not known exactly. However, at this

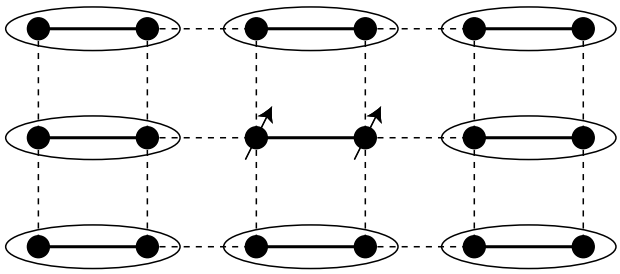

Figure 3: The triplon excitation of the $g > g_c$ paramagnet. The stationary triplon is an eigenstate only for $g = \infty$ but it becomes mobile for finite g.

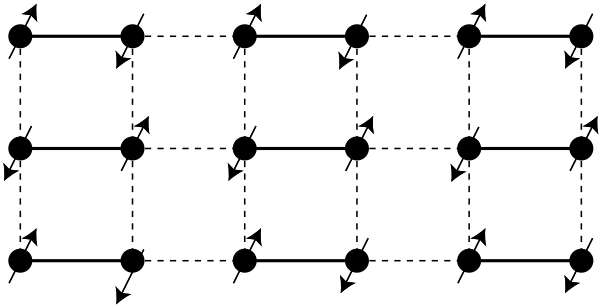

Figure 4: Schematic of the ground state with antiferromagnetic order with $g < g_c$.

point H_d becomes equivalent to the nearest-neighbor square lattice antiferromagnet, and this is known to have antiferromagnetic order in the ground state, as illustrated in Fig 4. This state is similar to the ferromagnetic ground state of H_I, with the difference that the magnetic moment now acquires a staggered pattern on the two sublattices, rather than the uniform moment of the ferromagnet. Thus in this ground state

$$\langle \mathrm{AF} | \, \hat{\sigma}_j^\alpha \, | \mathrm{AF} \rangle = N_0 \eta_j n_\alpha \tag{10}$$

where $0 < N_0 < 1$ is the antiferromagnetic moment, $\eta_j = \pm 1$ identifies the two sublattices in Fig 4, and n_α is an arbitrary unit vector specifying the orientation of the spontaneous magnetic moment which breaks the O(3) spin rotation invariance of H_d. The excitations above this antiferromagnet are also distinct from those of the paramagnet: they are a *doublet* of spin waves consisting of a spatial variation in the local orientation, n_α, of the antiferromagnetic order: the energy of this excitation vanishes in the limit of long wavelengths, in contrast to the finite energy gap of the triplon excitation

of the paramagnet.

As with H_I, we can conclude from the distinct characters of the ground states and excitations for $g \gg 1$ and $g \approx 1$ that there must be a quantum critical point at some intermediate $g = g_c$.

3 Quantum criticality

The simple considerations of Section 2 have given a rather complete description (based on the quasiparticle picture) of the physics for $g \ll g_c$ and $g \gg g_c$. We turn, finally, to the region $g \approx g_c$. For the specific models discussed in Section 2, a useful description is obtained by a method that is a generalization of the LGW method developed earlier for thermal phase transitions. However, some aspects of the critical behavior (*e.g.* the general forms of Eqns (13), (14), and (15)) will apply also to the quantum critical point of Section 4.

Following the canonical LGW strategy, we need to identify a collective order parameter which distinguishes the two phases. This is clearly given by the ferromagnetic moment in Eq. (4) for the quantum Ising chain, and the antiferromagnetic moment in Eq. (10) for the coupled dimer antiferromagnet. We coarse-grain these moments over some finite averaging region, and at long wavelengths this yields a real order parameter field ϕ_a, with the index $a = 1 \ldots n$. For the Ising case we have $n = 1$ and ϕ_a is a measure of the local average of N_0 as defined in Eq. (4). For the antiferromagnet, a extends over the three values x, y, z (so $n = 3$), and three components of ϕ_a specify the magnitude and orientation of the local antiferromagnetic order in Eq. (10); note the average orientation of a specific spin at site j is η_j times the local value of ϕ_a.

The second step in the LGW approach is to write down a general field theory for the order parameter, consistent with all symmetries of the underlying model. As we are dealing with a quantum transition, the field theory has to extend over *spacetime*, with the temporal fluctuations representing the sum over histories in the Feynman path integral approach. With this reasoning, the proposed partition function for the vicinity of the critical point takes the

following form

$$\mathcal{Z}_\phi = \int \mathcal{D}\phi_a(x,\tau) \exp\Big[- \int d^d x d\tau \left(\frac{1}{2} \left((\partial_\tau \phi_a)^2 + c^2 (\nabla_x \phi_a)^2 + s \phi_a^2 \right) + \frac{u}{4!} \left(\phi_a^2 \right)^2 \right) \Big]. \quad (11)$$

Here τ is imaginary time, there is an implied summation over the n values of the index a, c is a velocity, and s and $u > 0$ are coupling constants. This is a field theory in $d+1$ spacetime dimensions, in which the Ising chain corresponds to $d = 1$ and the dimer antiferromagnet to $d = 2$. The quantum phase transition is accessed by tuning the "mass" s: there is a quantum critical point at $s = s_c$ and the $s < s_c$ ($s > s_c$) regions corresponds to the $g < g_c$ ($g > g_c$) regions of the lattice models. The $s < s_c$ phase has $\langle \phi_a \rangle \neq 0$ and this corresponds to the spontaneous breaking of spin rotation symmetry noted in Eqs. (4) and (10) for the lattice models. The $s > s_c$ phase is the paramagnet with $\langle \phi_a \rangle = 0$. The excitations in this phase can be understood as small harmonic oscillations of ϕ_a about the point (in field space) $\phi_a = 0$. A glance at Eqn (11) shows that there are n such oscillators for each wavevector. These oscillators clearly constitute the $g > g_c$ quasiparticles found earlier in Eqn (7) for the Ising chain (with $n = 1$) and the triplon quasiparticle (with $n = 3$) illustrated in Fig 3) for the dimer antiferromagnet.

We have now seen that there is a perfect correspondence between the phases of the quantum field theory $\mathcal{Z}_\phi$ and those of the lattice models H_I and H_d. The power of the representation in Eqn. (11) is that it also allows us to get a simple description of the quantum critical point. In particular, readers may already have noticed that if we interpret the temporal direction τ in Eqn. (11) as another spatial direction, then $\mathcal{Z}_\phi$ is simply the classical partition function for a thermal phase transition in a ferromagnet in $d+1$ dimensions: this is the canonical model for which the LGW theory was originally developed. We can now take over standard results for this classical critical point, and obtain some useful predictions for the quantum critical point of $\mathcal{Z}_\phi$. It is useful to express these in terms of the dynamic susceptibility defined by

$$\chi(k,\omega) = \frac{i}{\hbar} \int d^d x \int_0^\infty dt \left\langle \left[\hat{\phi}(x,t), \hat{\phi}(0,0) \right] \right\rangle_T e^{-ikx + i\omega t}. \quad (12)$$

Here $\hat{\phi}$ is the Heisenberg field operator corresponding to the path integral in Eqn. (11), the square brackets represent a commutator, and the angular

brackets an average over the partition function at a temperature T. The structure of χ can be deduced from the knowledge that the quantum correlators of $\mathcal{Z}_\phi$ are related by analytic continuation in time to the corresponding correlators of the classical statistical mechanics problem in $d+1$ dimensions. The latter are known to diverge at the critical point as $\sim 1/p^{2-\eta}$ where p is the $(d+1)-$dimensional momentum, η is defined to be the anomalous dimension of the order parameter ($\eta = 1/4$ for the quantum Ising chain). Knowing this, we can deduce the form of the quantum correlator in Eq. (12) at the zero temperature quantum critical point

$$\chi(k,\omega) \sim \frac{1}{(c^2k^2-\omega^2)^{1-\eta/2}} \;\; ; \;\; T=0,\; g=g_c. \tag{13}$$

The most important property of Eq. (13) is the absence of a quasiparticle pole in the spectral density. Instead, $\mathrm{Im}\,(\chi(k,\omega))$ is non-zero for all $\omega > ck$, reflecting the presence of a continuum of critical excitations. Thus the stable quasiparticles found at low enough energies for all $g \neq g_c$ are absent at the quantum critical point.

We now briefly discuss the nature of the phase diagram for $T > 0$ with g near g_c. In general, the interplay between quantum and thermal fluctuations near a quantum critical point can be quite complicated, and we cannot discuss it in any detail here. However, the physics of the quantum Ising chain is relatively simple, and also captures many key features found in more complex situations, and is summarized in Fig 5. For all $g \neq g_c$ there is a range of low temperatures ($T \lesssim |g-g_c|$) where the long time dynamics can be described using a dilute gas of thermally excited quasiparticles. Further, the dynamics of these quasiparticles is quasiclassical, although we reiterate that the nature of the quasiparticles is entirely distinct on opposite sides of the quantum critical point. Most interesting, however, is the novel *quantum critical* region, $T \gtrsim |g-g_c|$, where neither quasiparticle picture nor a quasiclassical description are appropriate. Instead, we have to understand the influence of temperature on the critical continuum associated with Eq. (13). This is aided by scaling arguments which show that the only important frequency scale which characterizes the spectrum is $k_BT/\hbar$, and the crossovers near this scale are universal *i.e.* independent of specific microscopic details of the lattice Hamiltonian. Consequently, the zero momentum dynamic susceptibility in the quantum critical region takes the following form at small frequencies:

$$\chi(k=0,\omega) \sim \frac{1}{T^{2-\eta}} \frac{1}{(1-i\omega/\Gamma_R)}. \tag{14}$$

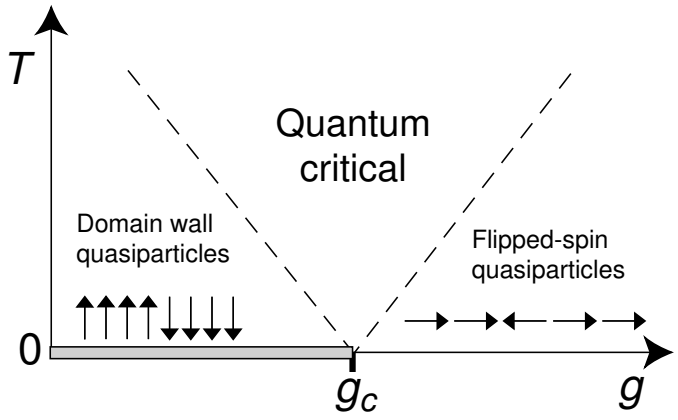

Figure 5: Nonzero temperature phase diagram of H_I. The ferromagnetic order is present only at $T = 0$ on the shaded line with $g < g_c$. The dashed lines at finite T are crossovers out of the low T quasiparticle regimes where a quasiclassical description applies. The state sketched on the paramagnetic side used the notation $|{\rightarrow}\rangle_j = 2^{-1/2}(|{\uparrow}\rangle_j + |{\downarrow}\rangle_j)$ and $|{\leftarrow}\rangle_j = 2^{-1/2}(|{\uparrow}\rangle_j - |{\downarrow}\rangle_j)$.

This has the structure of the response of an overdamped oscillator, and the damping frequency, Γ_R, is given by the universal expression

$$\Gamma_R = \left(2 \tan \frac{\pi}{16}\right) \frac{k_B T}{\hbar} \tag{15}$$

The numerical proportionality constant in Eqn. (15) is specific to the quantum Ising chain; other models also obey Eqn. (15) but with a different numerical value for this constant.

4 Beyond LGW theory

The quantum transitions discussed so far have turned to have a critical theory identical to that found for classical thermal transitions in $d + 1$ dimensions. Over the last decade it has become clear that there are numerous models, of key physical importance, for which such a simple classical correspondence does not exist. In these models, quantum *Berry phases* are crucial in establishing the nature of the phases, and of the critical boundaries between them. In less technical terms, a signature of this subtlety is an important simplifying feature which was crucial in the analyses of Section 2: both models

had a straightforward $g \to \infty$ limit in which we were able to write down a simple, non-degenerate, ground state wavefunction of the 'disordered' paramagnet. In many other models, identification of the 'disordered' phase is not as straightforward: specifying absence of a particular magnetic order is not enough to identify a quantum state, as we still need to write down a suitable wavefunction. Often, subtle quantum interference effects induce new types of order in the 'disordered' state, and such effects are entirely absent in the LGW theory.

An important example of a system displaying such phenomena is the $S = 1/2$ square lattice antiferromagnet with additional frustrating interactions. The quantum degrees of freedom are identical to those of the coupled dimer antiferromagnet, but the Hamiltonian preserves the full point-group symmetry of the square lattice:

$$H_s = \sum_{j<k} J_{jk} \left(\hat{\sigma}_j^x \hat{\sigma}_k^x + \hat{\sigma}_j^y \hat{\sigma}_k^y + \hat{\sigma}_j^z \hat{\sigma}_k^z \right) + \ldots \tag{16}$$

Here the $J_{jk} > 0$ are short-range exchange interactions which preserve the square lattice symmetry, and the ellipses represent possible further multiple spin terms. Now imagine tuning all the non-nearest-neighbor terms as a function of some generic coupling constant g. For small g, when H_s is nearly the square lattice antiferromagnet, the ground state has antiferromagnetic order as in Fig 4 and Eqn. (10). What is now the 'disordered' ground state for large g? One natural candidate is the spin-singlet paramagnet in Fig 2. However, because all nearest neighbor bonds of the square lattice are now equivalent, the state in Fig 2 is degenerate with 3 other states obtained by successive 90 degree rotations about a lattice site. In other words, the state in Fig 2, when transferred to the square lattice, *breaks* the symmetry of lattice rotations by 90 degrees. Consequently it has a new type of order, often called valence-bond-solid (VBS) order. It is now believed that a large class of models like H_s do indeed exhibit a second-order quantum phase transition between the antiferromagnetic state and a VBS state—see Fig 6. Both the existence of VBS order in the paramagnet, and of a second-order quantum transition, are features that are not predicted by LGW theory: these can only be understood by a careful study of quantum interference effects associated with Berry phases of spin fluctuations about the antiferromagnetic state. We will not enter into details of this analysis here, but will conclude our discussion by writing down the theory so obtained for the quantum critical

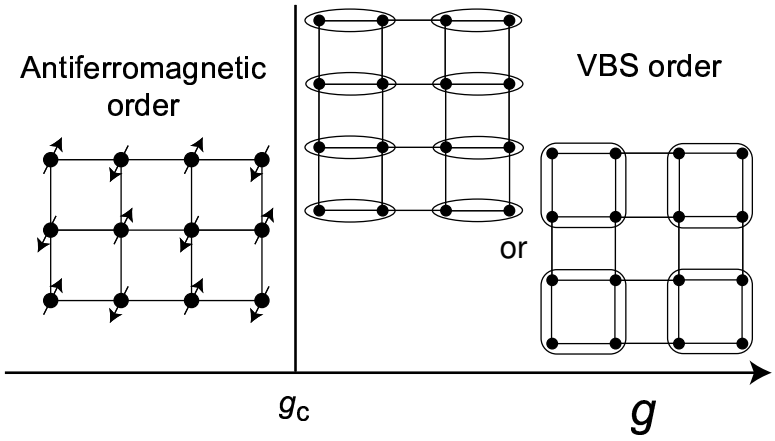

Figure 6: Phase diagram of H_s. Two possible VBS states are shown: one which is the analog Fig 2, and the other in which spins form singlets in a plaquette pattern. Both VBS states have a four-fold degeneracy due to breaking of square lattice symmetry. So the novel critical point at $g = g_c$ (described by $\mathcal{Z}_z$) has the antiferromagnetic and VBS orders vanishing as it is approached from either side: this co-incident vanishing of orders is generically forbidden in LGW theories.

point in Fig 6:

$$\mathcal{Z}_z = \int \mathcal{D}z_\alpha(x,\tau)\mathcal{D}A_\mu(x,\tau)\exp\Bigg(-\int d^2x d\tau\Big[|(\partial_\mu - iA_\mu)z_\alpha|^2 + s|z_\alpha|^2 + \frac{u}{2}(|z_\alpha|^2)^2 + \frac{1}{2e^2}(\epsilon_{\mu\nu\lambda}\partial_\nu A_\lambda)^2\Big]\Bigg). \tag{17}$$

Here μ, ν, λ are spacetime indices which extends over the 2 spatial directions and τ, α is a *spinor* index which extends over $\uparrow$, $\downarrow$, and z_α is complex spinor field. In comparing $\mathcal{Z}_z$ to $\mathcal{Z}_\phi$, note that the vector order parameter ϕ_a has been replaced by a spinor z_α, and these are related by $\phi_a = z^*_\alpha \sigma^a_{\alpha\beta} z_\beta$, where σ^a are the Pauli matrices. So the order parameter has *fractionalized* into the z_α. A second novel property of $\mathcal{Z}_z$ is the presence of a U(1) gauge field A_μ: this gauge force emerges near the critical point, even though the underlying model in Eqn (16) only has simple two spin interactions. Studies of fractionalized critical theories like $\mathcal{Z}_c$ in other models with spin and/or charge excitations is an exciting avenue for further theoretical research.

References

[1] Sachdev, Subir (1999), *Quantum Phase Transitions*. Cambridge: Cambridge University Press.

[2] Matsumoto, M., Yasuda, C., Todo, S., and Takayama, H, Physical Review B **65**, 014407 (2002).

[3] Senthil, T., Balents, L., Sachdev, S., Vishwanath, A., and Fisher, M. P. A., http://arxiv.org/abs/cond-mat/0312617.